

Social adaptive behavior and oscillatory prevalence in an epidemic model on evolving random geometric graphs

Akhil Panicker^{1,*} and V. Sasidevan^{1,†}

¹*Department of Physics, Cochin University of Science and Technology, Kochi, 682022 Kerala, India*
(Dated: March 31, 2022)

Our recent experience with COVID19 amply shows that spatial effects like mobility and average interpersonal distance are very important in deciding the outcome of an epidemic dynamics. Spatial connectivity structure of a population is usually modelled via Random Geometric Graphs which are networks generated from spatially distributed components where connections between components are made based on a distance-dependent probability measure. Structural and dynamical aspects of such graphs are important in describing processes with a spatial dependence such as the spread of an airborne disease. In this work, using a simple computational model of an epidemic, we investigate how spatial factors like average separation between individuals and their mobility affect the spread of a disease. We show that such spatial factors can give rise to oscillatory prevalence in a society of adaptive individuals. We also show that delays in executing non-pharmaceutical spatial mitigation strategies can accentuate oscillatory prevalence and can have non-monotonic effects on the peak prevalence. In both cases, we characterize the effects of different parameters on the prevalence of the disease and peak infection and obtain threshold values.

PACS numbers:

INTRODUCTION

Epidemics have always been a threat to humanity from ancient times. The black death wiped out two-thirds of the European population in 13th century [1]. COVID19 has so far caused more than 6 million deaths [2]. Understanding and controlling such events are therefore of paramount importance for our own survival on earth. The dynamics of epidemics have been analyzed using various types of mathematical and computational models. Such models are of immense importance as they can give us quantitative insights into the dynamic process of an epidemic. Together with the knowledge generated in various other disciplines and field data, models help us to make informed decisions to effectively deal with a pandemic. Information gained from models of epidemic which incorporate pharmaceutical and non-pharmaceutical interventions are important in order to have a better control over the epidemic [3–6].

The major type of mathematical models of epidemic is the compartmental models in which a population is divided into various compartments such as S (Susceptible), I (Infected), R (Recovered), etc based on the state of infection of individuals. In the simplest setting, such models constitute a set of rate equations for the fraction of individuals in various compartments and are mean-field in nature [7–9]. Real-world population structures are different from the ones typically considered in the mean-field equations of compartmental models. In a more realistic setting, population structure is modelled as a network in which individuals are the nodes and connections are the links of a complex network. In the network, two individuals are assumed to be ‘connected’ if the disease can be transmitted between them. Models of epidemic spread on such topological networks have been extensively investigated in the past [10–12].

In many real world settings, spatial factors such as the average distance between individuals and their mobility play a crucial part in deciding the structure of a contact network and will influence any dynamic process defined on such a network. The networks where the connectivity is decided by a distance-dependent measure are called random geometric graphs [13, 14]. Such spatial factors which are normally not considered in epidemic models on topological networks has gained increased recent attention in the wake of the COVID19 pandemic [15–20]. In such spatial network models of epidemic, individuals or nodes are embedded in 2D space in which connections exist between two nodes only if they are closer than a characteristic distance or the transmission range of a disease. The value of the characteristic distance can vary from zero for a disease which transmits only by person-to-person direct contact up to several meters for airborne diseases. So the structure of the contact network will be disease-dependent. Models of epidemic on spatial networks can give us valuable insights into the dynamics of a disease in a population by incorporating factors like mobility of individuals, mask-usage and other distance-dependent intervention strategies.

Various pharmaceutical and non-pharmaceutical intervention strategies can be employed to control an epidemic. For an air-born disease like COVID19, mask usage, social-distancing and mobility restrictions are some of the most important non-pharmaceutical techniques that can be used to control the epidemic. Such intervention actions will have a direct bearing on the contact structure of the population [21–29]. Mask usage will reduce the ‘connectivity’

of the network by reducing the transmission range of viral particles between persons. Social distancing and mobility restrictions will also reduce the connectivity or the mean degree of the network by keeping individuals apart as in a low-density population. Since the effect of all such intervention actions are effectively the same viz, reduction of connectivity of the network, we will refer to all such actions by the generic term ‘Social Adaptation’ (SA). Previous works which incorporate similar social adaptation have shown that oscillations in prevalence can arise due to individual payoff-based game-theoretic considerations by the agents [30–34].

In this work, we investigate how the adoption of such non-pharmaceutical intervention strategies by the agents who are spatially distributed and are mobile, affects the outcome of an SIR dynamics. The connectivity structure of agents is modeled by random geometric graphs which evolves by the adaptive actions of individuals as well as their mobility. The adaptive action of agents is incorporated via a threshold model for social adaptation i.e. their decision to follow SA depends upon the level of global prevalence with respect to a threshold prevalence. We show that such adaptive actions by the agents can give rise to oscillations in the prevalence of the disease even with a simple SIR dynamics. We quantitatively characterize the effectiveness of non-pharmaceutical intervention strategies in controlling the epidemic. We obtain conditions under which effective reduction in the peak prevalence can be obtained from numerical solutions as well as simulations. We also study the effect of delays in executing such non-pharmaceutical SA strategies on the epidemic. In this case we show that such delays accentuates oscillations in the prevalence and has a non-monotonic effect on the peak prevalence. Our study shows how spatial factors like mobility and average interpersonal distance together with the adaptive actions of the population - either voluntary or enforced- can give rise to epidemic waves in time.

The paper is organized as follows. In Sec. , we introduce SIR model on evolving random geometric graphs and discuss its threshold behavior. We characterize the effect of mobility of agents on the SIR dynamics. In Sec. , we discuss the effect of non-pharmaceutical adaptive strategies by the agents on the dynamics of the epidemic and how that leads to oscillations in the prevalence. In Sec. , we consider the effects of delays in implementing the mitigation strategies followed by a discussion of our results in Sec. .

SIR DYNAMICS ON EVOLVING RANDOM GEOMETRIC GRAPHS

We will follow the works of [30, 35, 36] in defining an epidemic model with spatially distributed agents. We consider a spatial network in which N individuals (nodes) are distributed uniformly and randomly in a square patch of length L with density ρ . The density of agents is given by $\rho = \frac{N}{L^2}$. Two nodes are assumed to be ‘connected’ and can potentially pass on the disease if they are closer than a characteristic transmission range b . At each time step, agents move and assume new positions randomly in the square patch and hence a new connectivity structure forms. SIR dynamics is implemented on this evolving RGG at each time step where Susceptible (S), Infected (I) and Recovered (R) are the compartments. Over time, all the individuals interact with all others so that one can write down mean-field equations to model the process. Let β be the probability with which infection is transmitted to a neighbor of an infected individual and γ be the probability that an infected individual recovers from infection in any time step. At any time step t , the number of Susceptible, Infected and Recovered agents are denoted by $S(t)$, $I(t)$, $R(t)$ such that

$$S(t) + I(t) + R(t) = N \quad (1)$$

or

$$s(t) + i(t) + r(t) = 1 \quad (2)$$

Where $s(t) = S(t)/N$, $i(t) = I(t)/N$, $r(t) = R(t)/N$ are the normalized values of the number of Susceptible, Infected and Recovered agents respectively. Now the probability of a susceptible agent not being infected by any of its infectious neighbors in a given time step is $(1 - \beta)^n$ where $n = \rho\pi b^2 i(t)$ is the average number of infected neighbors inside a disk of radius b . Therefore, the equations for the evolution of the fraction of agents in different compartments take the form,

$$s(t+1) = s(t) - s(t)[1 - (1 - \beta)^{\pi b^2 \rho i(t)}] \quad (3)$$

$$i(t+1) = i(t) - \gamma i(t) + s(t)[1 - (1 - \beta)^{\pi b^2 \rho i(t)}] \quad (4)$$

$$r(t+1) = r(t) + \gamma i(t) \quad (5)$$

For small values of β , Eq. 4 can be approximated as,

$$i(t+1) \approx i(t) - \gamma i(t) + [1 - i(t) - r(t)]\beta\pi b^2 \rho i(t) \quad (6)$$

Since the recovered compartment $r(t)$ will be very small at the beginning of an epidemic, letting $r(t) \rightarrow 0$, Eq. 6 becomes,

$$i(t+1) \approx i(t) - \gamma i(t) + [1 - i(t)]\beta\pi b^2 \rho i(t) \quad (7)$$

Therefore for the epidemic to grow, we must have,

$$1 - \gamma + \beta\pi b^2 \rho \geq 1 \quad (8)$$

Thus for a given density, the critical characteristic transmission range for an outbreak to happen is given by

$$b_{epi} = \sqrt{\frac{\gamma}{\rho\pi\beta}} \quad (9)$$

For values of b above b_{epi} , epidemic outbreak happens and below it, epidemic cannot happen, a condition which replaces the usual condition based on the reproductive number $R_0 > 1$ for the spread of an epidemic [35, 36]. It is instructive to compare the above critical range with that for the formation of a giant connected component in the system. The latter can be obtained by realizing that the connectivity structure in the present problem is the same as that in a continuum percolation of overlapping discs with radius b . Denoting the critical radius of discs by b_{gc} , we know that [37]

$$b_{gc} \approx \sqrt{\frac{1.128}{\pi\rho}} \quad (10)$$

In a population with no mobility, b_{gc} will act as a lower threshold value of the characteristic transmission range below which no epidemic spread can occur. However, when there is mobility, the lower threshold is given by Eq. 9. We have the relation

$$b_{epi} = b_{gc} \sqrt{\frac{\gamma}{1.128\beta}} \quad (11)$$

Fig.1 shows the variation of the critical characteristic range b_{epi} with the density of the population. For a given value of β and γ , such a curve demarcates epidemic and non-epidemic regions. In the present work, we will use the values, transmission probability (β) = 0.5 and recovery rate (γ) = 0.05. This means that there is a 50% chance that a susceptible person who is within the characteristic range of an infected person will get the disease and the average number of days for recovery is 20. Changing these values do not affect the qualitative nature of the results.

Fig. 2 shows the prevalence over time curves for the cases with and without mobility of agents. The mobility of agents has a pronounced effect on both the peak prevalence and the duration of the epidemic. We can see that the peak prevalence more than doubled when the agents are fully mobile.

Note that for a given disease, both β and γ are fixed quantities over which we do not have any control in general. So the only controllable parameters here are the characteristic range b and the density of agents ρ . Characteristic range b may be altered by measures such as mask usage while ρ may be altered by measures such as social distancing or lock-downs. Note that a change in b can also be viewed as a corresponding change in the density ρ . Fig. 3 shows the variation of peak prevalence with the characteristic range. Again, we compare the results with the case in which there is no mobility. The cases without and with full mobility act as the extreme scenarios and we can anticipate an intermediate behavior in case of a population with intermediate values for mobility.

EFFECT OF SPATIAL INTERVENTION STRATEGIES ON THE EPIDEMIC

An effective non-pharmaceutical intervention strategy to contain a disease like COVID19 which can transmit from person to person via air is to reduce the average effective interpersonal distance in a population. Measures such as mask-usage, promoting social-distancing, or partial or complete lock-downs are all examples of such strategies. Such measures could be either self-imposed by the agents or imposed by an external agency. Such measures are usually imposed and removed depending on the prevalence of the disease in the population although this mayn't be the

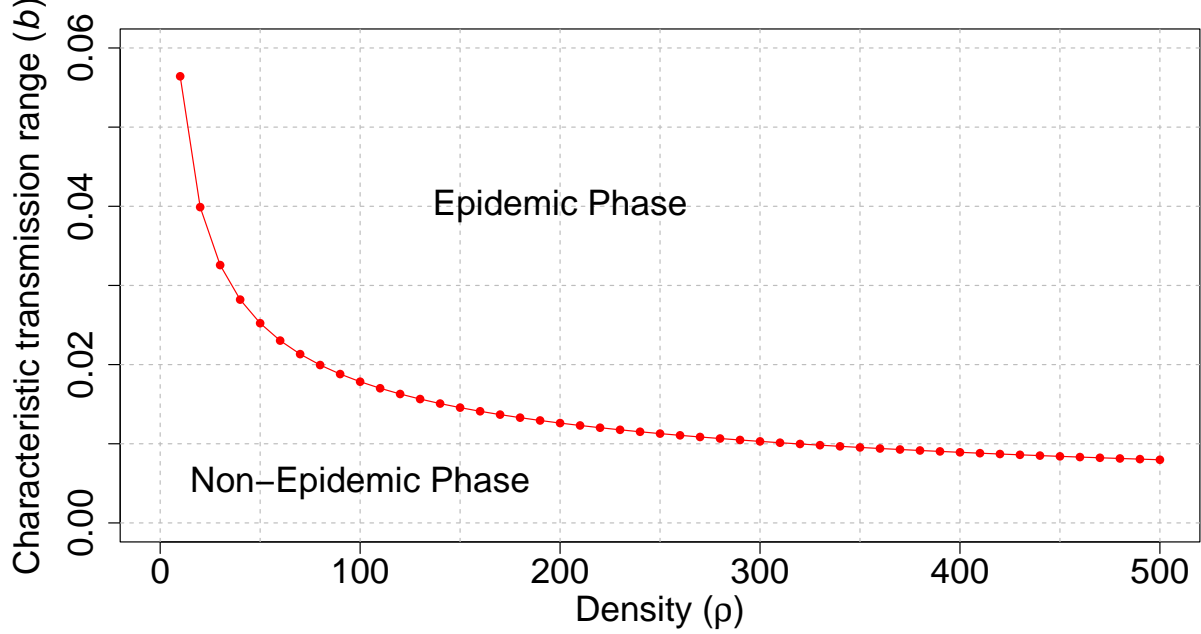


Figure 1: **Variation of critical characteristic transmission range with density.** Critical characteristic range is calculated using Eq. 9 for different values of density. Throughout the present work, we will use the values transmission probability (β) = 0.5 and recovery rate (γ) = 0.05. Epidemic outbreak is forbidden in the region below the red line whereas it is allowed above it.

sole criteria based on which such decisions are made. Ideally we would like such strategies to have the effect that the average Euclidean distance between the individuals in the population becomes greater than the characteristic transmission range of the disease. For a given disease, we may view non-pharmaceutical intervention strategies as to either **(a)** Increase the average distance between the agents or **(b)** Reduce the transmission range of the disease b . The first method can be implemented by assuming that the length of the system is increased by a factor of f while keeping the number of agents the same when the agents follow social-adaptation such that mean-distance between individuals increases by a factor of f where $f \geq 1$. So the density changes from $\rho = \frac{N}{L^2}$ to $\rho^{SA} = \frac{N}{(Lf)^2}$ where ρ^{SA} is the density of the agents while following social-adaptation strategies. The second method can be implemented by assuming that the characteristic transmission range b is reduced by a factor of $1/f$. While both methods are mathematically same, the latter describes situations like using face masks which effectively reduce the transmission range of the disease. In this work, we will employ reduction of b to implement SA and will call f as the SA factor.

We assume that agents or a central agency monitors the level of global prevalence in the population. Whenever the epidemic prevalence go above a pre-defined threshold value c , agents follow social distancing from the next time step till the prevalence is reduced below the threshold (See Fig. 4). The characteristic transmission range b then evolves according to,

$$b(t+1) = \begin{cases} \frac{b(t)}{f}, & \text{if } i(t) > c \\ b(t), & \text{otherwise} \end{cases} \quad (12)$$

where $b(0)$ is the original characteristic transmission range of the disease in the absence of any SA. The mean degree of the network thus assumes either of the two values $\rho\pi b^2$ and $\frac{1}{f^2}\rho\pi b^2$ depending upon the prevalence at any time step.

Fig. 5 gives a comparison of the prevalence with and without SA. As we increase the SA factor f , the peak infection continues to drop, but a significant drop in the peak infection is achieved only beyond a critical value of f ($f \approx 6$ in the figure). This can be understood based on the fact that for lower values of f , there is still an effective giant cluster in the system aiding the epidemic to spread. In other words, SA is not enough to bring the system below the critical

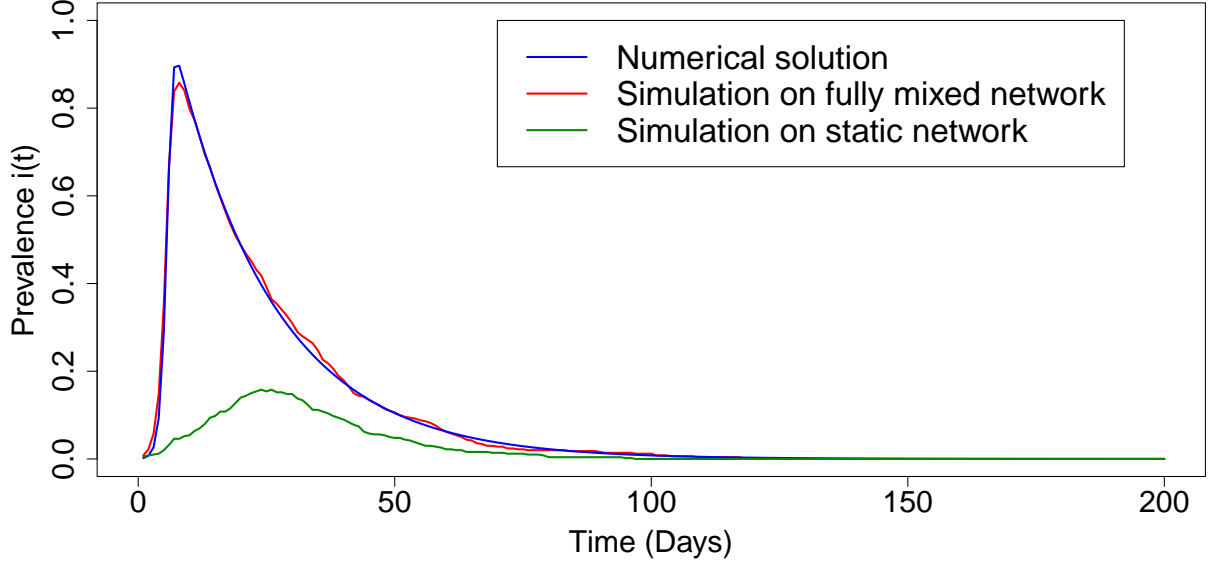


Figure 2: **Variation of prevalence over time.** Prevalence $i(t)$ is plotted for numerical and simulated solutions of epidemic with mobility. Prevalence is also shown for the case where the agents are not mobile. Characteristic range $b = 0.05$ and density $\rho = 500$.

line in Fig. 1. As the value of f go beyond the critical value, we can see that the prevalence oscillates around the threshold value c which indicates that the characteristic transmission range went below its critical value. The critical value of f say f_c is related to the critical value of the characteristic transmission range b_{epi} by

$$f_c = b_{epi} \sqrt{\frac{\rho\pi\beta}{\gamma}} \quad (13)$$

Fig. 6 shows the variation of peak infection with the SA factor f . As we increase the value of f , peak infection reduces till a critical value of f and thereafter the peak infection stagnates. A further increase of f is not effective in reducing the peak infection and is not optimal from a socio-economic point of view as it imposes additional restrictions on the population without any additional benefits.

It is instructive to look at the peak infection as a function of the initial characteristic transmission range $b(0)$ for different values of the social distancing factor f which is shown in Fig. 7. We can see that the peak infection becomes non-zero above the critical threshold given by Eq. 13. However for a particular value of f , the peak infection is contained at the threshold value c for a range of values of $b(0)$. As we further increase $b(0)$, the adaptation is no longer effective in controlling the epidemic and the peak infection again rises after a specific value of $b(0)$. For higher values of f , the range over which the peak infection remains at the threshold value is also higher. The behavior can be understood based on the critical characteristic range b_{epi} given in Eq. 9. The peak prevalence is contained at the threshold c only when the adaptation brings the effective interpersonal distance to values below b_{epi} .

We further extent the model to include a lower threshold for removal of the social adaptation as well. Fig. 8 gives a comparison of the prevalence with and without SA with upper threshold and a lower threshold. As we increase the SA factor f , the peak infection continues to drop, but a significant drop in the peak infection is achieved only beyond a critical value of f ($f \approx 4$ in the figure). Here, whenever the adaptation factor is large enough to reduce the characteristic transmission range to values below its critical value, oscillations in prevalence are seen with bigger amplitudes lying between the threshold values.

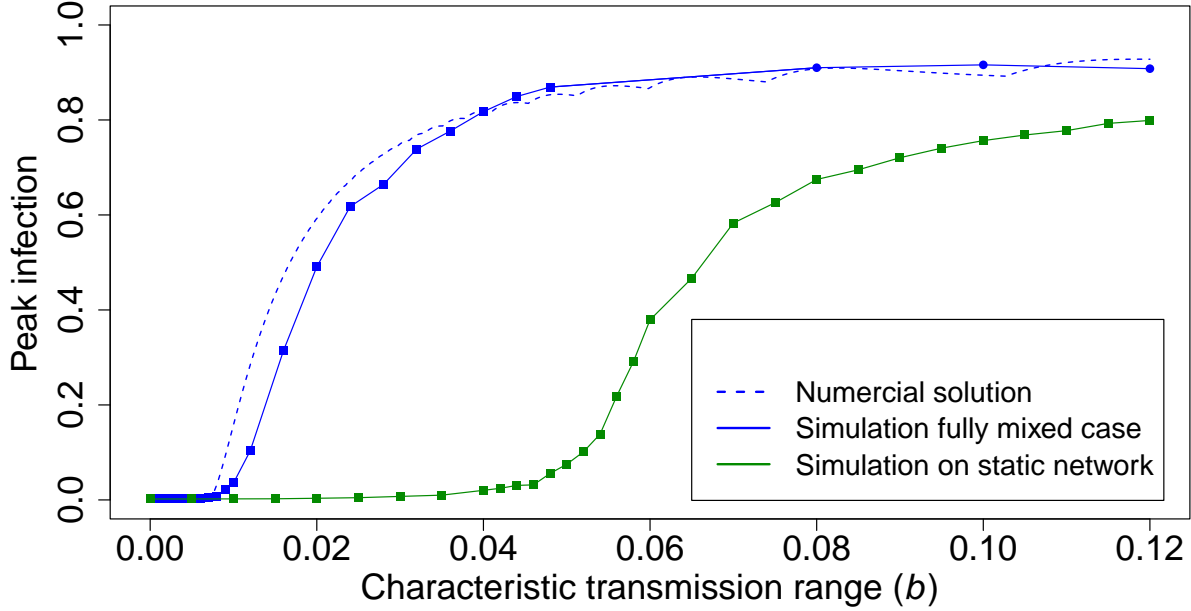


Figure 3: **Variation of peak infection with characteristic transmission range.** Variation of peak infection with characteristic range b is shown for static and fully mixed spatial networks. Simulation results are compared with numerical solutions. Density $\rho = 500$.

EFFECT OF DELAY IN IMPLEMENTING SOCIAL ADAPTATION

So far we have assumed that the adaptive action by the agents is implemented without any delay. So whenever the prevalence crosses the threshold, the agents adapt in the very next time step. However, in practice, it is more likely that such adaptive action happens with a hold up due to a delay in the transmission of information about global prevalence or due to implementation delays. To account for such effects, we introduce a delay parameter so that if the prevalence goes above or below the threshold in a particular time step, the adaptive action by the agents happens only after a delay of d time steps. We can imagine that such a delay can play a significant role in deciding the outcome of any attempt in controlling an epidemic. For highly contagious diseases, this delay can lead to situations where infection has already affected a significant fraction of the population even before information about global prevalence is available or any preventive action is taken. For a delay of d time steps, we have

$$b(t + 1 + d) = \begin{cases} \frac{b(t)}{f}, & \text{if } i(t) > c \\ b(t), & \text{otherwise} \end{cases} \quad (14)$$

In Fig. 9 we show the prevalence for various values of the delay parameter d . We can see that as the delay increases, peak infection rises significantly and after a critical value of delay, adaptation becomes irrelevant. We can also see that bigger oscillations in the prevalence occur due to the combined effect of the social adaptation and the delay. Corresponding peak infection curves are shown in Fig. 10. We can clearly see the non-monotonic effect of a delay especially for larger values of the characteristic transmission range. This is especially important because it shows the importance of implementing preventive measures with minimum delay especially for diseases with higher values of transmission range.

DISCUSSION AND CONCLUSION

Spatial effects like mobility and average interpersonal distance are very important in deciding the outcome of an epidemic dynamics as amply shown by our recent experience with COVID19. A number of recent works have discussed

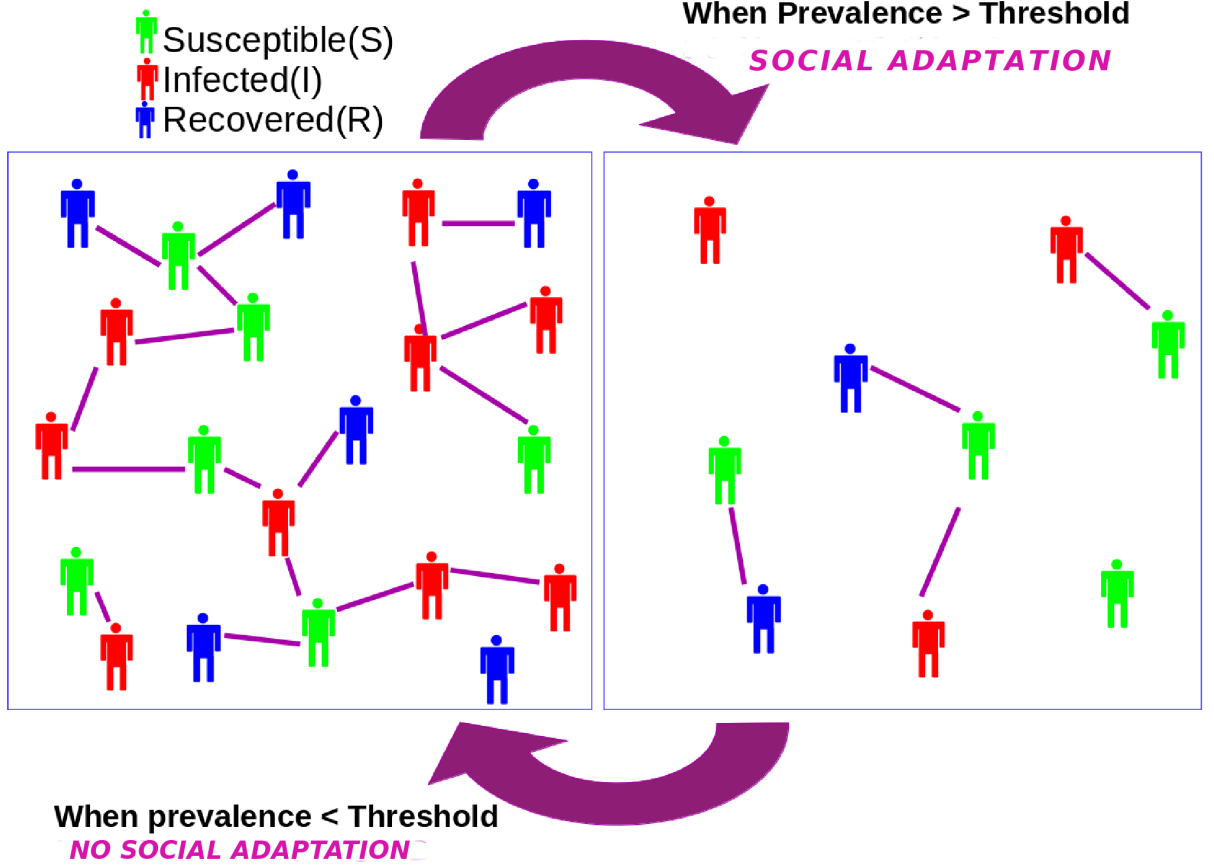


Figure 4: **Schematic representation of the adaptive behavior of agents in the model.** Agents employ social adaptation whenever the global prevalence of the disease is greater than a threshold c and discard it otherwise.

the effects of including the spatial aspects in the dynamic of an epidemic with adaptive agents [30, 31, 33, 34]. In general we can use the framework of Random Geometric Graphs for modeling the spread of an epidemic incorporating spatial factors. Mobility of agents is incorporated by considering such graphs as evolving. In this work, we extended such models and considered agents who sense the global prevalence of the epidemic and take adaptive measures. Agents follow and discard social adaptation based on predefined prevalence thresholds. Our results show that such adaptation can have a significant effect on the trajectory of the epidemic dynamics. We characterize how different levels of adaptation by the agents affect the prevalence of the disease and the peak level of infection. Oscillatory prevalence is seen for a range of values of the adaptation parameter f . Our results also show that a delay in implementing the adaptation can have non-monotonic effects on peak prevalence which shows quantitatively that monitoring the global prevalence levels accurately is very crucial so that early intervention based on such information is possible. In particular, delay in disseminating information and/or delay in taking adaptive measures can accentuate oscillatory prevalence. Our results show that how simple adaptation behavior by the agents can lead to waves during an epidemic even with SIR model.

An important theme which is evident when spatial factors are included is that the usual condition of reproduction number $R_0 = \beta/\gamma > 1$ for an epidemic outbreak may be replaced by the more general condition $1 - \gamma + \beta\pi b^2\rho > 1$ where ρ is the density of the population and b is the characteristic transmission range of a disease. The latter condition helps to differentiate between factors that can be easily attributed to the disease itself (like γ , β and b) and factors related to how the agents are distributed over space (like the density ρ or the average distance between the agents in the population). Since we can control the latter via various non-pharmaceutical strategies like social distancing, mask wearing, partial or complete lock down etc, the condition thus helps us to clearly define the target criteria in order to contain the propagation of a disease.

In this work, we considered extreme scenarios where the agents either mix fully spatially at each time step or do

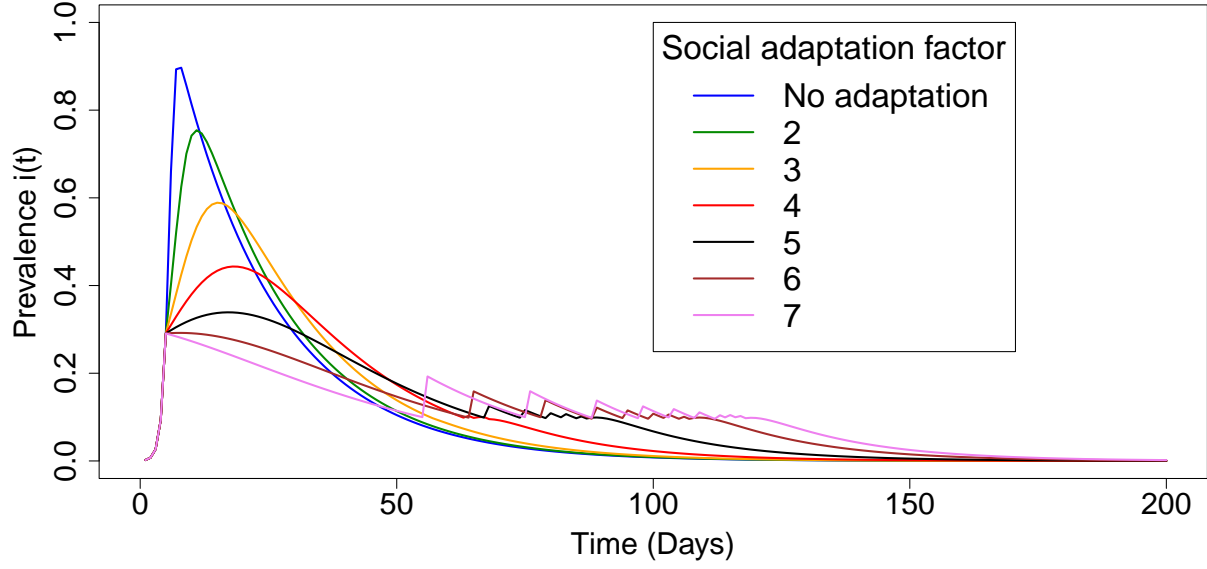


Figure 5: **Numerical solution of prevalence as a function of time for various values of social adaptation factor f .** $f = 1$ corresponds to the case with no adaptive measures employed. Density $\rho = 500$. Initial characteristic transmission range $b(0) = 0.05$.

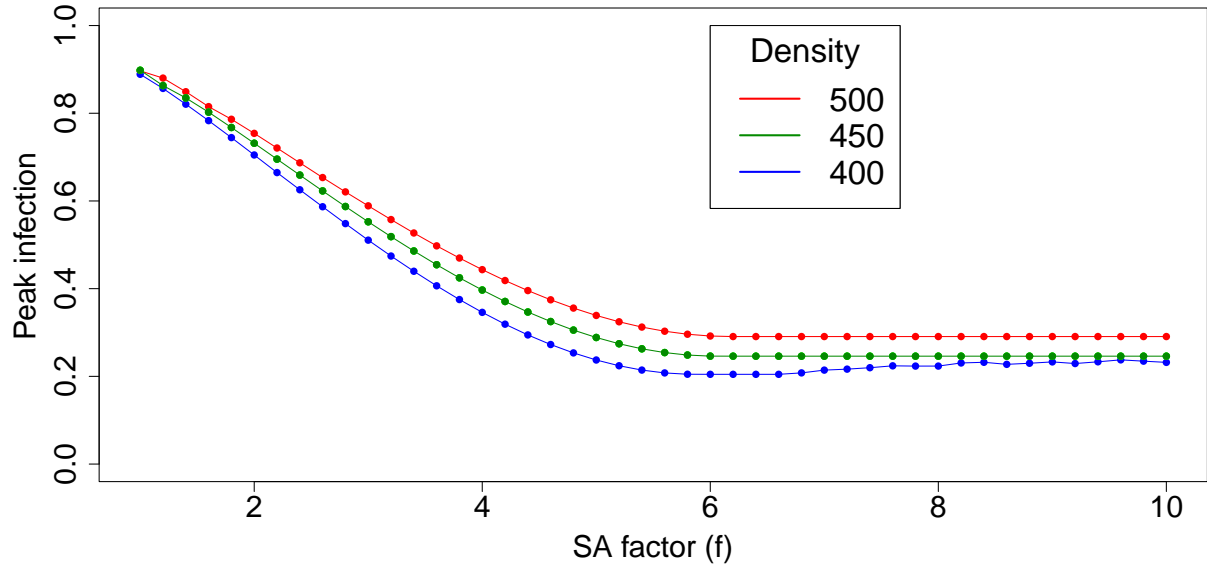


Figure 6: **Numerical solution for variation of peak infection with social distancing factor f for various values of densities ρ and initial characteristic transmission range $b(0)$.** Threshold $c = 0.1$.

not mix at all. We can easily extend the setting to consider situations where the mixing of agents is more gradual and/or limited spatially. A more realistic setting may be the one in which several patches of individuals are connected together by a few long range connections with full mixing within each patch [38]. We may also introduce heterogeneity in the population by considering distributions for parameters characterizing social adaptation, prevalence threshold, and mobility [39]. This is especially relevant for mobility as infected individuals will in general be less mobile. Another

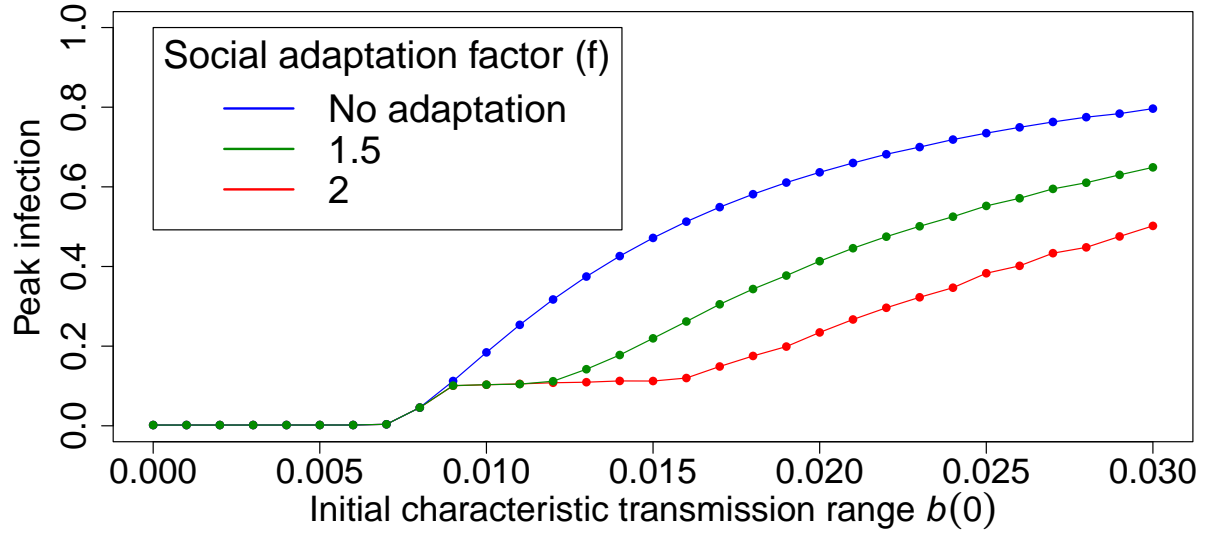


Figure 7: Numerical solution for variation of peak infection with initial characteristic transmission range $b(0)$ for various values of social adaptation factor f . Threshold $c = 0.1$.

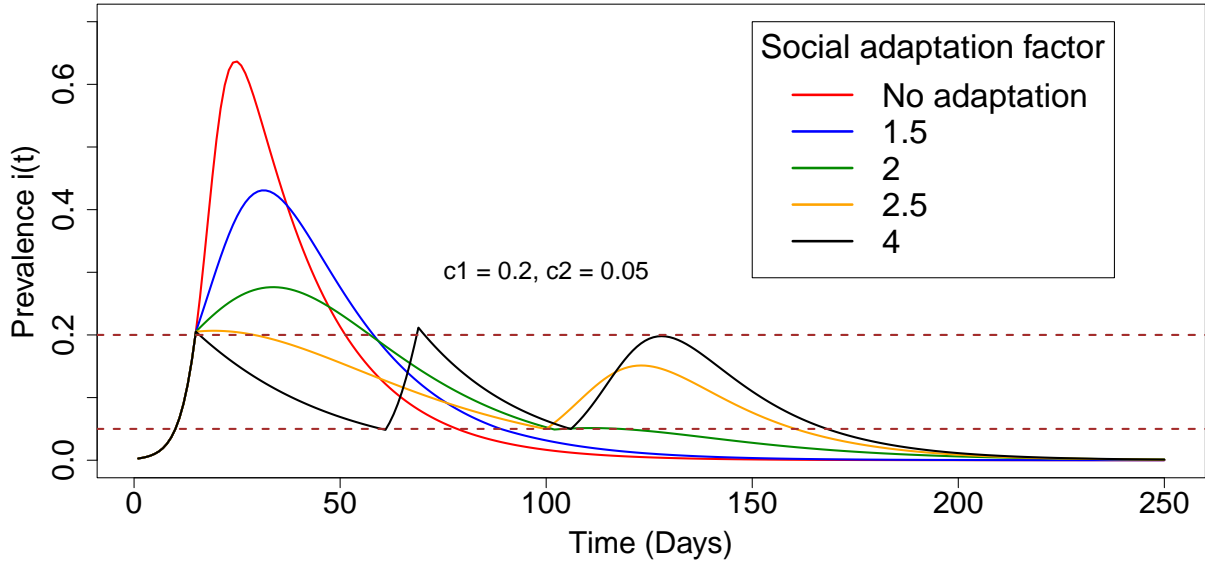


Figure 8: Numerical solution of prevalence as a function of time for various values of social adaptation factor f . $f = 1$ corresponds to the case with no adaptive measures employed. Density $\rho = 500$, initial characteristic transmission range $b(0) = 0.02$. $c1 = 0.2$ is the upper threshold and $c2 = 0.05$ is the lower threshold.

obvious direction for future work is to consider the role of spatial adaptation in other models of epidemic like SEIR. Finally, it will be interesting to look at the effect of social adaptation based on local information about the epidemic rather than the global one as considered in the present work. Going further, strategizing agents may be considered who will try to optimize individual adaptive actions based on information about the prevalence and the action of other agents [40]. We will explore some of these avenues in a future work.

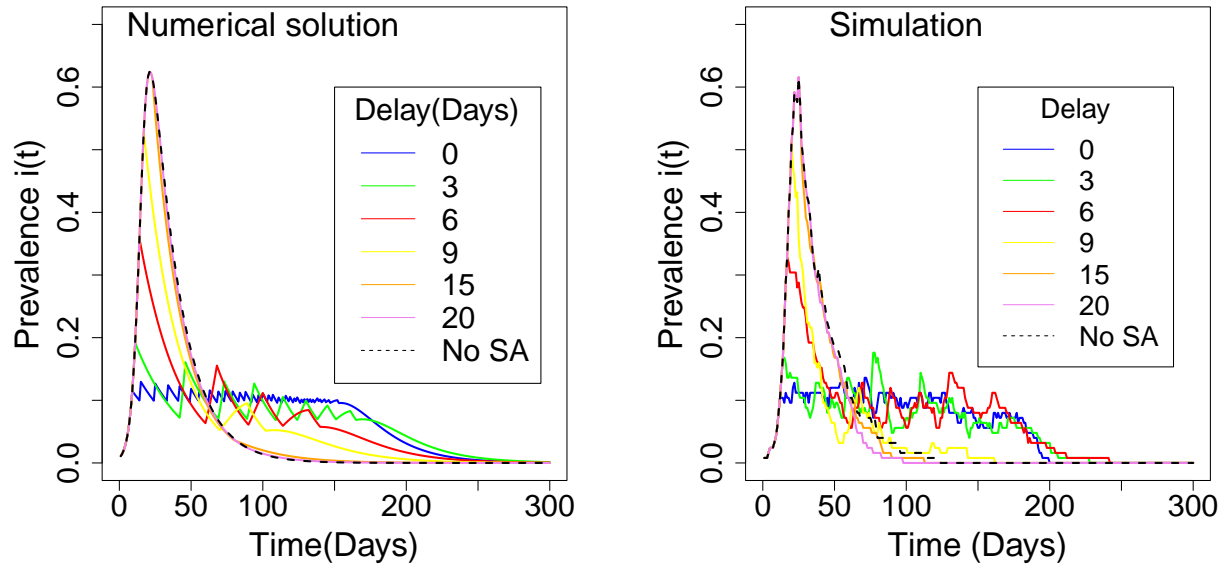


Figure 9: **Variation of prevalence with time when there is a delay of d time steps in implementing and removing SA.** Results from numerical solution and simulation are shown. Threshold $c = 0.1$, initial characteristic transmission range $b(0) = 0.05$, and density $\rho = 500$.

* Electronic address: atpanicker95@gmail.com

† Electronic address: sasidevan@cusat.ac.in, sasidevan@gmail.com

- [1] Austin Alchon, Suzanne. A pest in the land: new world epidemics in a global perspective. University of New Mexico Press: 21: 2003: ISBN 0-8263-2871-7.
- [2] Coronavirus database. accessed 28 Feb 2022: <https://www.worldometers.info/coronavirus/>
- [3] Ahmed, Danish A. et al. Mechanistic modelling of COVID-19 and the impact of lockdowns on a short-time scale. PLOS ONE: 10: 16: 1-20: 2021.
- [4] Gatto, M. et al. Spread and dynamics of the Covid-19 epidemic in Italy: Effects of emergency containment measures. Proc. Natl. Acad. Sci. USA: 117: 10484-10491: 2020.
- [5] Colizza, V., Barrat, A., Barthélemy, M., Valleron, A.-J. & Vespignani, A. Modeling the worldwide spread of pandemic influenza: Baseline case and containment interventions. PLoS Med: 117: 4: e17: 2007.
- [6] Lang, John C et al. Analytic models for SIR disease spread on random spatial networks. Journal of Complex Networks: 6: 6: 948-970: 2018.
- [7] Ottar N Bjornstad. Epidemics, Models and Data using R. Springer International Publishing.: 2018.
- [8] Keeling MJ, Rohani P. Modeling infectious diseases in humans and animals. Princeton University Press: 2008.
- [9] Rothman, Kenneth J et al. Modern epidemiology. Wolters Kluwer Health/Lippincott Williams & Wilkins Philadelphia: 3: 2008.
- [10] Pastor-Satorras, R, Castellano, C., Van Mieghem, & P. Vespignani. Epidemic processes in complex networks. Rev. Mod. Phys: 87: 925: 2015.
- [11] Cohen, Reuven and Havlin, Shlomo. Complex networks: structure, robustness and function. Cambridge university press: 2010.
- [12] Turner, S., Klimek, P. Hanel, R.. A network-based explanation of why most covid-19 infection curves are linear. Proc. Natl. Acad. Sci. USA: 117:22684-22689: 2020.
- [13] Barthélemy, Marc. Spatial networks. Physics Reports: 499(1-3): 1- 101: 2011.
- [14] Mathew Penrose. Random Geometric Graphs. Oxford Scholarship Online: ISBN-13: 9780198506263.
- [15] Thomas, Loring J et al. Spatial heterogeneity can lead to substantial local variations in COVID-19 timing and severity. Proc. Natl. Acad. Sci. U.S.A: 117: 24180-24187: 2020
- [16] Wong, David WS et al. Spreading of COVID-19: Density matters. Plos one: 15: 12: e0242398; 2020
- [17] Chang, Serina et al. Mobility network models of COVID-19 explain inequities and inform reopening. Nature: 589: 7840: 82-87: 2021
- [18] Pujari, Bhalchandra S and Shekatkar, Snehal M. Multi-city modeling of epidemics using spatial networks: Application to

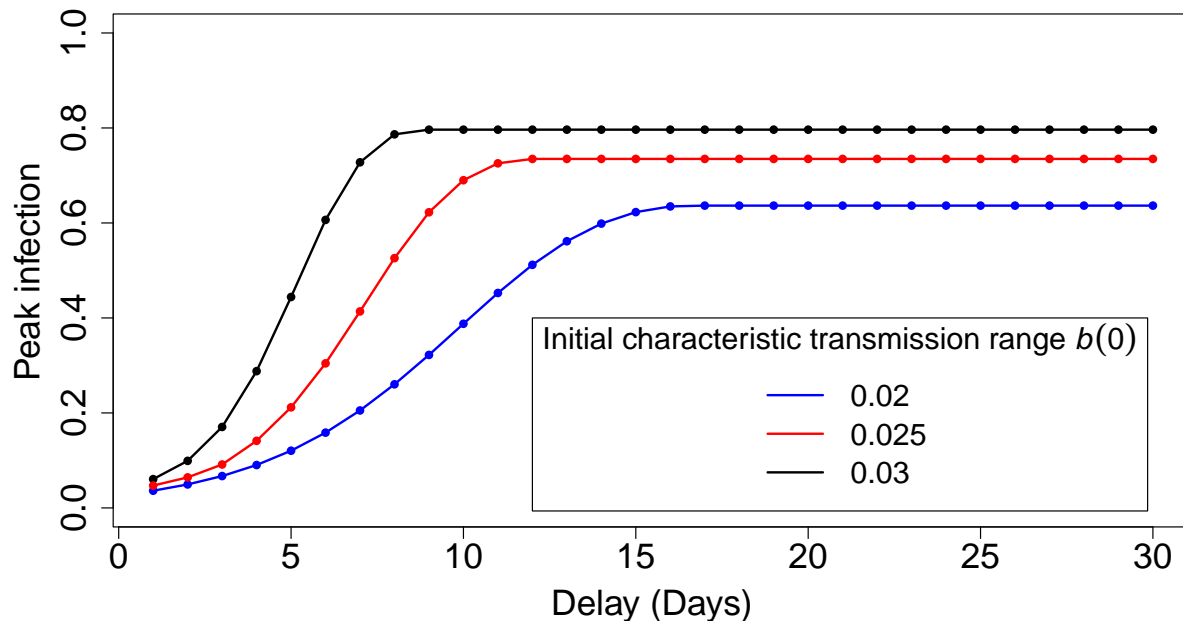


Figure 10: **Variation of peak infected fraction with the delay parameter d for various values of initial characteristic transmission range $b(0)$.** Threshold $c = 0.1$, density $\rho = 500$, social adaptation factor $f = 4$.

2019-nCov (COVID-19) coronavirus in India. Medrxiv: 2020

- [19] Melin, Patricia et al. Analysis of spatial spread relationships of coronavirus (COVID-19) pandemic in the world using self organizing maps. *Chaos, Solitons & Fractals*: 138: 109914: 2020.
- [20] Kang, Dayun et al. Spatial epidemic dynamics of the COVID-19 outbreak in China. *International Journal of Infectious Diseases*: 94: 96 – 102: 2020.
- [21] te Vrugt, M., Bickmann, J. Wittkowski, R. Effects of social distancing and isolation on epidemic spreading modeled via dynamical density functional theory. *Nat. Commun*: 11: 5576: 2020.
- [22] Maier, B. F. & Brockmann, D. Effective containment explains sub exponential growth in recent confirmed covid-19 cases in china. *Science*: 368: 742-746: 2020.
- [23] Nowak B, Brzoska P et al. Adaptive Human Behavior in Epidemiological Models. *Proc. Natl. Acad. Sci. USA*: 03: 108: 6306-6311: 2011.
- [24] Arthur RF, Jones JH, Bonds MH, Ram Y, Feldman MW. Adaptive social contact rates induce complex dynamics during epidemics. *PLOS Computational Biology*: 17: 2: e1008639: 2021.
- [25] Havlin, Shlomo. Epidemic spreading and control strategies in spatial modular network. *Applied Network Science*: 95: 5: 1: 2020.
- [26] Paulo Cesar Ventura et al. Epidemic spreading in populations of mobile agents with adaptive behavioral response. *Chaos, Solitons and Fractals*: 156: 111849: 2022.
- [27] Lopez, Leonardo et al. The end of social confinement and COVID-19 re-emergence risk. *Nature Human Behaviour*: 4: 7: 746-755: 2020.
- [28] Funk, Sebastian et al. The spread of awareness and its impact on epidemic outbreaks. *Proc. Natl. Acad. Sci. USA*: 106: 16: 6872 - 6877: 2009.
- [29] Caley P, Philp DJ, McCracken K. Quantifying social distancing arising from pandemic influenza. *Journal of the Royal Society Interface*: 5: 23: 631-9: 2008.
- [30] Glaubitz Alina and Fu Feng. Oscillatory dynamics in the dilemma of social distancing. *Proc. R. Soc. A*: 67- 78: 2020.
- [31] H. Khazaei, K. Paarporn, A. Garcia and C. Eksin. Disease spread coupled with evolutionary social distancing dynamics can lead to growing oscillations. 2021 60th IEEE Conference on Decision and Control (CDC): 4280-4286: 2021.
- [32] Jianping Huang, Xiaoyue Liu et al. The oscillation-outbreaks characteristic of the COVID-19 pandemic . *National Science Review*: 8: 2021.
- [33] Just W, Saldana J, Xin Y. Oscillations in epidemic models with spread of awareness. *J Math Biol*: 76: 4: 1027-1057: 2018.
- [34] Liu Haoyan, Wang Xin, Liu Longzhao, Li Zhoujun. Co-evolutionary Game Dynamics of Competitive Cognitions and Public Opinion Environment . *Frontiers in Physics*: 9: 2021.

- [35] A. Buscarino et al. Disease spreading in populations of moving agents. *Europhysics Letters*: 82: 3: 38002: 2008.
- [36] Peng, Xiao-Long et al. An SIS epidemic model with vaccination in a dynamical contact network of mobile individuals with heterogeneous spatial constraints. *Commun. Nonlinear Sci. Numer. Simulat*: 73: 52 – 73: 2019.
- [37] Mertens, Stephan and Moore, Cristopher et al. Percolation threshold of a two-dimensional continuum system. *Phys. Rev. E*: 86: 6: 061109: 2012.
- [38] F.E. Cornes and G.A. Frank and C.O. Dorso. COVID-19 spreading under containment actions. *Physica A*: 588: 126566: 2022
- [39] G. Ellison. Implications of heterogeneous SIR models for analyses of COVID-19. tech. rep., National Bureau of Economic Research, 2020.
- [40] Sharma, Anupama et al. Epidemic prevalence information on social networks can mediate emergent collective outcomes in voluntary vaccine schemes. *PLOS Computational Biology*: 15: 5: 2019.